ELSEVIER

Polymer 40 (1999) 801–805

polymer

Polymer Communication

A d.s.c. study of crystallization behaviour of poly(α-*n*-alkyl β-L-aspartate)s

Y. Calventus[a], P. Colomer[a], J. Málek[1a], S. Montserrat[a,*], F. López-Carrasquero[c], A. Martínez de Ilarduya[b], S. Muñoz-Guerra[b]

[a]*Departament de Màquines i Motors Tèrmics, ETSEIT, Universitat Politècnica de Catalunya (UPC), Colom 11, E-08222 Terrassa, Spain*
[b]*Departament d'Enginyeria Química, ETSEIB, UPC, Diagonal 647, E-08028 Barcelona, Spain*
[c]*Universidad de los Andes, Departamento de Química, Facultad de Ciencias, Mérida 5101A, Venezuela*

Revised 3 March 1998

Abstract

A series of poly(α-*n*-alkyl β-L-aspartate)s (where *n* is the number of carbon atoms in the linear alkyl side chain, with $n = 12$, 18 and 22), was studied by differential scanning calorimetry. The effect of the length of alkyl side chain on the non-isothermal crystallization kinetics on cooling was investigated. It was found that the ΔH_c and crystallization rate of PAALA samples on cooling increase with the alkyl side chain length. A similar trend is observed for the activation energy of the crystallization process. It was found that the Johnson–Mehl–Avrami model cannot be applied for a quantitative description of non-isothermal d.s.c. data corresponding to this crystallization process.

Keywords: Non-isothermal crystallization; Poly(α-*n*-alkyl β-L-aspartate)s d.s.c.

1. Introduction

The poly(α-*n*-alkyl β-L-aspartate)s are a series of novel comb-like polyamides derived from nylon 3, whose chemical structure is as shown the following:

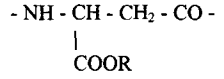

R being the alkyl group of the side chain. These polymers are here called PAALA-*n*, where *n* represents the number of carbon atoms contained in the alkyl group. These polymers are closely related to the poly(γ-alkyl α-L-glutamate)s largely studied in recent years [1–5].

Recent studies carried out in the poly(α-*n*-alkyl β-L-aspartate)s have shown that the formation of helical structures seems to be a common property of these compounds [6–8]. PAALA-*n*, with $n \geq 12$, tends to organize into two-dimensional biphasic structures with main chain helices and alkyl side chains distributed into two separate domains [9]. The alkyl side chains are able to crystallize between the layered structure of main chain helix originating phase A. The melting of the ordered side chains originates phase B [9,10]. Fig. 1 shows a schematic model illustrating the structural changes in PAALA-18 when the transition B → A takes place. The interlayer distance changes from 2.8 to 3.1 nm.

The aim of this work is a non-isothermal study of this crystallization process (transition B → A) by differential scanning calorimetry (d.s.c.) in PAALA-*n*, with $n \geq 12$. Non-isothermal crystallization data of similar processes in polymers are usually described using the Johnson–Mehl–Avrami (JMA) model [11,12]. It is well known, however, that this theoretical model has been developed for the description of isothermal crystallization [13,14], and its validity can be extended to non-isothermal applications only if the crystals of a new phase grow from a constant number of nuclei and all nucleation is completed prior to macroscopic crystal growth [14–16]. The aim of this paper is to test the applicability of the JMA model for the description of the non-isothermal crystallization process of PAALA-*n* samples.

2. Kinetic analysis

The heat flow, ϕ, generated during the crystallization process can be described by the following equation [17]:

$$\phi = \Delta H_c A \, e^{-E/RT} f(\alpha) \quad (1)$$

* Corresponding author.
[1] Permanent address: Joint Laboratory of Solid State Chemistry, Acad. Sci. of the Czech Republic and University of Pardubice, Studentská 84, 530 09 Pardubice, Czech Republic.

0032-3861/98/$ - see front matter
PII S0032-3861(98)00200-6

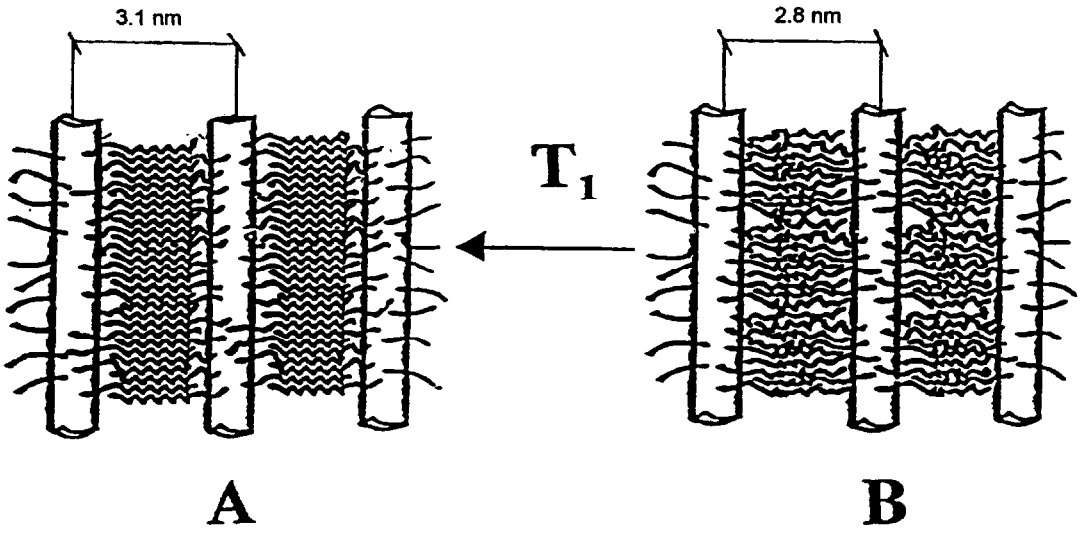

Fig. 1. Schematic model illustrating the structural changes taking place in PAALA-*n*, with $n \geq 12$, during the crystallization process on cooling.

where ΔH_c is the crystallization heat, A is the pre-exponential factor and E is the effective activation energy. This parameter can be calculated from the slope of the plot of logarithm of heat flow at a given fractional conversion α, plotted against the reciprocal temperature as follows from the logarithmic form of Eq. (1):

$$\ln \phi_\alpha = \ln[\Delta H_c A \cdot f(\alpha)] - E/RT \tag{2}$$

The function $f(\alpha)$ represents the mathematical expression for the kinetic model. The JMA equation [11,12] is probably the most frequently used model for the description of crystallization kinetics. Usually it is represented in the following form [17].

$$f(\alpha) = n(1-\alpha)[-\ln(1-\alpha)]^{1-1/n} \tag{3}$$

This model, however, was derived in isothermal conditions and its applicability for non-isothermal data should be carefully checked [14–16]. This can be done, e.g. using two special functions defined as follows [18].

$$y(\alpha) = \phi \cdot e^{E/RT} \tag{4}$$

$$z(\alpha) = \phi \cdot T^2 \tag{5}$$

For practical reasons these functions are normalized within the $\langle 0,1 \rangle$ interval. It was shown by Málek [16] that the maximum of the function $z(\alpha)$ (usually labelled α_p^∞) has characteristic values for a particular kinetic model. For the JMA model this maximum should be close to $\alpha_p^\infty = 0.632$.

The $y(\alpha)$ function is proportional to the kinetic model function $f(\alpha)$, as follows from comparison of Eq. (1) and Eq. (4). Therefore, the shape of normalized $y(\alpha)$ plot is characteristic for the kinetic model and it can be used as a diagnostic probe for kinetic model determination. There are

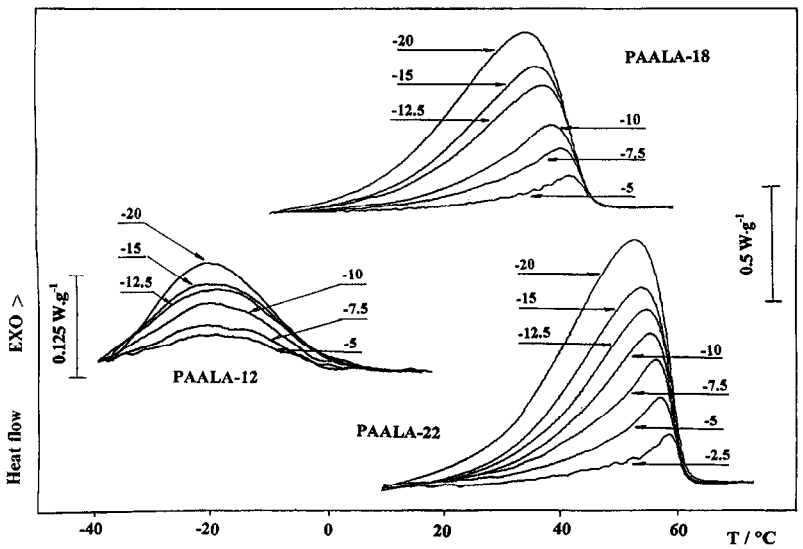

Fig. 2. D.s.c. curves of PAALA-*n* samples for the indicated alkyl side chain length. Different cooling rates in K min^{-1} are indicated by numbers.

Table 1
Temperatures of onset (T_{on}) and peak maximum (T_p) at different cooling rates β for the PAALA-n samples

β (K min^{-1})	PAALA-12		PAALA-18		PAALA-22	
	T_{on} (°C)	T_p (°C)	T_{on} (°C)	T_p (°C)	T_{on} (°C)	T_p (°C)
−2.5	—	−11.5	45.2	41.1	60.5	57.8
−5	3.8	−17.3	45.2	39.7	60.5	56.8
−7.5	2.4	−14.7	45.2	37.8	60.5	56.2
−10	2.3	−18.3	45.2	36.9	60.5	55.4
−12.5	5.7	−15.6	45.2	36.8	60.5	54.6
−15	5.4	−17.5	45.2	35.4	60.5	53.4
−20	6.1	−19.2	45.2	33.1	60.5	52.5

two possibilities for the JMA model [18]. If the $y(\alpha)$ function has a maximum at $\alpha_M = 0$, then it can be linear for $n = 1$ or concave for $n < 1$. If the $y(\alpha)$ function exhibits a maximum in the interval $\alpha_M \in (0,\alpha_p)$ (where α_p is the fractional conversion at the maximum of the d.s.c. peak) then it corresponds to a $n > 1$ model. The mathematical condition for the maximum then can be expressed as follows:

$$\alpha_p^{\infty} = 1 - \exp\left(\frac{1}{n} - 1\right) \tag{6}$$

An alternative method of testing the applicability of the JMA model is based on the shape index analysis of the d.s.c. curve and it is explained in detail elsewhere [16].

3. Experimental

3.1. Materials

The poly(α-n-alkyl β-L-aspartate)s used in this work, i.e. PAALA-12, -18 and -22, were prepared by non-assisted anionic ring-opening polymerization of the corresponding optically pure (*S*)-4-(alkoxycarbonyl)-2-azetidinones [9]. This method allows to obtain these polymers for a wide range of n values with a high degree of stereoregularity and large molecular weights.

3.2. Measurements

Calorimetric measurements were performed with a Mettler TA-4000 thermoanalyzer equipped with a low temperature range DSC-30 differential scanning calorimetric module and with a Mettler DSC 821e with faster response and higher resolution. The instruments were previously calibrated with indium standard. The samples were heated from 10 to 120°C at 10 K min^{-1} and left at this temperature for 5 min. Then, the samples were cooled at constant rate ranging between 2.5 and 20 K min^{-1} from 120 to −20°C in order to crystallize the molten paraffinic side chain. Samples weights of about 6 mg were used in all the experiments.

4. Results and discussion

Fig. 2 shows d.s.c. curves corresponding to the non-isothermal crystallization of PAALA-n samples at various cooling rates measured using the DSC-30 instrument. The PAALA-12 crystallizes in the temperature range between 20 and −35°C, PAALA-18 in the range between 55 and −10°C and PAALA-22 in the range between 70 and 10°C. The extrapolated onset temperature of the crystallization peak, T_{on}, is practically identical and independent on the cooling rate for PAALA-18 and 22 (45.2 and 60.5°C, respectively), while there are some differences (lower than 3°C) in PAALA-12 (see Table 1). Likewise, the initial slope of the d.s.c. curves until the maximum of the crystallization peak is very pronounced, and therefore the crystallization rate seems to be very fast, particularly in PAALA-18 and 22. These facts allow to suppose that the nucleation and growth processes are probably overlapped. No significative differences were observed using the DSC-821e instrument with faster response.

As is evident, the crystallization enthalpy increases with the length of the alkyl chain. The values of ΔH_c are summarized in Table 2. Little difference is observed between the crystallization enthalpy values for PAALA-18

Table 2
The parameters characterizing the crystallization process in studied materials

Sample	$-\Delta H_c$ (J g^{-1})	E (kJ mol^{-1})	α_M	α_p^{∞}
PAALA-22	69 ± 2	318 ± 20	0	0.23 ± 0.04
PAALA-18	50 ± 2	191 ± 15	0.07 ± 0.02	0.26 ± 0.03
	55 ± 2[a]	202 ± 33	0.11 ± 0.08	0.25 ± 0.03
PAALA-12	26 ± 1	128 ± 47	0	0.41 ± 0.05

[a]Measured by the DSC 821e instrument

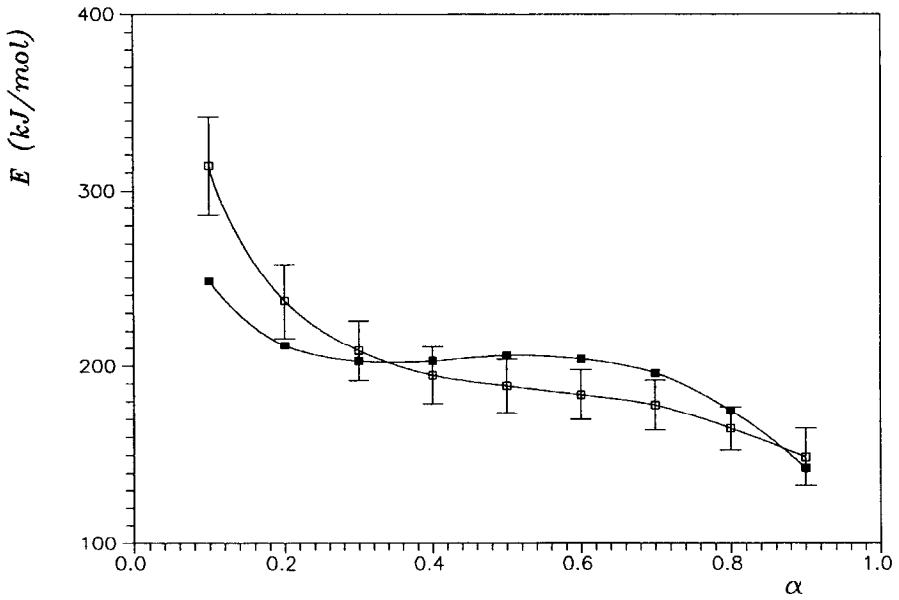

Fig. 3. The activation energy of PAALA-18 sample as a function of fractional conversion α. The points were calculated by the isoconversional method using Eq. (2) for non-isothermal data obtained by the Mettler DSC-30 (□) and DSC-821e (■) instruments. The lines are drawn as guide for the eye.

between the DSC-821e and DSC-30 ($55 \pm 2\ J\ g^{-1}$ and $50 \pm 2\ J\ g^{-1}$, respectively). The crystallized fraction at the temperature of the maximum of the peak, α_p, is very low (<0.35) and changes with the sample and with the cooling rate.

Fig. 3 shows the activation energy for the PAALA-18 calculated using Eq. (2) for experimental data obtained by the DSC-30 and DSC-821e instruments as a function of the fractional conversion α. The value of E is practically constant (within 10% error limit) except for the peak tails, and their average values calculated in the range $0.3 \leq \alpha \leq 0.7$ are shown in Table 2. The average value of the activation energy increases with the length of the alkyl side chains n. This increase can be attributed to the greater mobility acquired by side chains, which acts as an obstacle for their interaction, making the crystallization process more difficult.

Using these values of the activation energy for the different PAALA-n, the $y(\alpha)$ function can be calculated using Eq. (4). These functions (normalized within the ⟨0,1⟩ interval) calculated for various cooling rates are plotted as points in Fig. 4 for PAALA-18. Theoretical $y(\alpha)$ functions

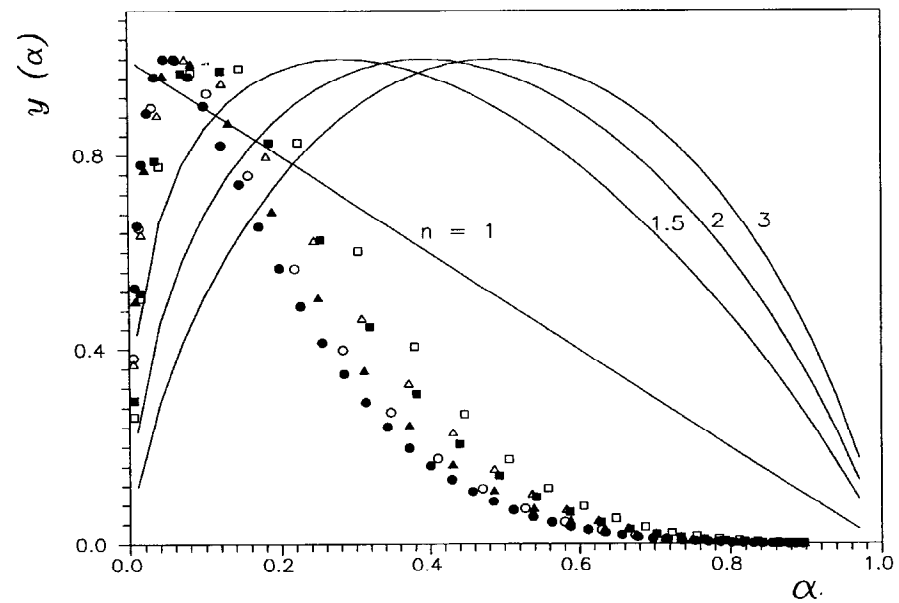

Fig. 4. The $y(\alpha)$ function for the PAALA-18 sample calculated using Eq. (4) for various non-isothermal experiments: (□) 2.5; (■) 5; (△) 7.5; (▲) 12.5; (○) 15; and (●) 20 K min^{-1}. Full lines correspond to normalized $f(\alpha)$ functions calculated for the JMA model using Eq. (3).

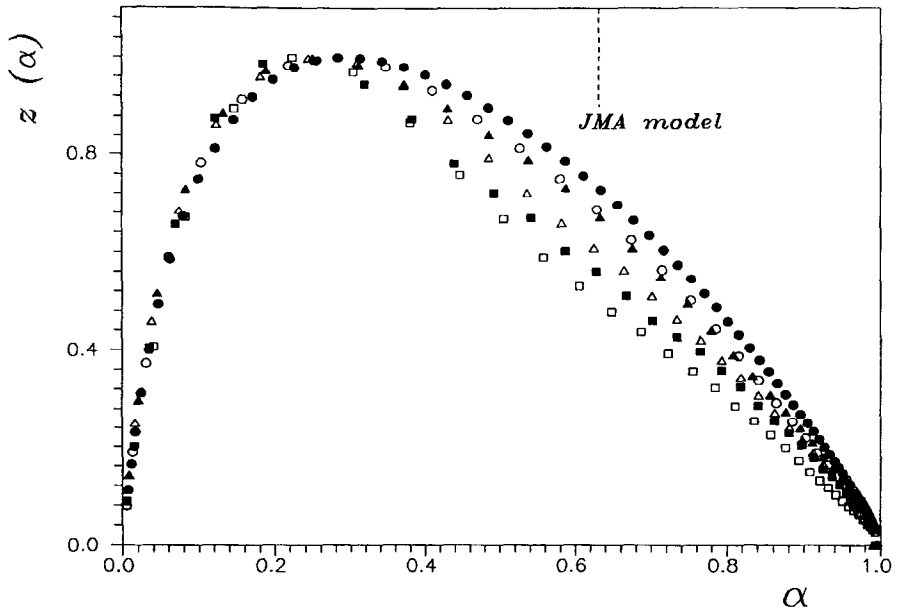

Fig. 5. The $z(\alpha)$ function for the PAALA-18 sample calculated using Eq. (5) for various non-isothermal experiments: (□) 2.5; (■) 5; (△) 7.5; (▲) 12.5; (○) 15; and (●) 20 K min^{-1}. The value of α_p^∞ typical for the JMA model is marked with broken line.

calculated for various values of kinetics exponent $n = 1$, 1.5, 2 and 3 for JMA model are shown by full lines. It is clear that the experimental data cannot be described by the JMA model. The values of α_M (see Table 2) are approximately 0 in PAALA-12 and 22 and 0.1 for PAALA-18.

The plot of $z(\alpha)$ function calculated using Eq. (5) versus α for PAALA-18 is shown in Fig. 5. This function exhibits a maximum at $\alpha_p^\infty = 0.632$ independently of the kinetic exponent and the activation energy. The α_p^∞ value for this sample is 0.26, which is considerably lower than the 0.632 corresponding to the JMA model (broken line). Similar behaviour was observed also for PAALA-12 and PAALA-22 (see Table 2). These facts indicate that the calorimetric data obtained from the non-isothermal crystallization of these samples cannot be described by the JMA model.

For values higher than 0.3 the $z(\alpha)$ function shifts with cooling rate. This is probably due to the thermal inertia effect of the instrument as a consequence of the extremely fast crystallization process. It seems, therefore, that quantitative analysis of the non-isothermal crystallization with determination of the kinetic parameters is not possible in this case.

5. Conclusions

It was found that the ΔH_c and crystallization rate of PAALA samples, on cooling, increase with the alkyl side chain length. A similar trend is observed for the activation energy of the crystallization process. It was found that the Johnson–Mehl–Avrami model cannot be applied for a quantitative description of non-isothermal d.s.c. data corresponding to this crystallization process.

Acknowledgements

Financial support was provided by DGICYT (Project number: PB 93/1241). One of the authors (J.M.) wish to acknowledge financial assistance for a sabbatical period at UPC from the Ministerio de Educación y Ciencia.

References

[1] Daly WH, Poché D, Negulescu II. Prog Polym Sci 1994;19:79.
[2] Watanabe J, Ono H, Uematsu I, Abe A. Macromolecules 1985;18:2141.
[3] Watanabe J, Ono H. Macromolecules 1986;19:1079.
[4] Yamanabe T. Macromolecules 1988;21:48.
[5] Romero Colomer FJ, Gómez Ribelles JL, Llovera Maciá J, Muñoz Guerra S. Polymer 1991;32 (9):1642.
[6] López Carrasquero F, Martínez de Ilarduya A, Muñoz Guerra S. Polym J 1994;26:694.
[7] López Carrasquero F, Alemán C, Garcia Alvarez M, Martínez de Ilarduya A, Muñoz Guerra S. Makromol Chem Phys 1995;196:253.
[8] López Carrasquero F, Garcia Alvarez M, Muñoz Guerra S. Polymer 1994;35:4502.
[9] López Carrasquero F, Montserrat S, Martínez de Ilarduya A, Muñoz Guerra S. Macromolecules 1995;28:5535.
[10] Montserrat S, Colomer P, Calventus Y, López Carrasquero F, Martínez de Ilarduya A, Muñoz Guerra S. J Therm Anal 1997;49:693.
[11] Johnson WA, Mehl RF. Trans Am Inst Miner Eng 1939;135:416.
[12] Avrami MJ. Phys Chem 1939;7:1103.
[13] Henderson DW. J Therm Anal 1979;15:325.
[14] Henderson DW. J Non-Cryst Solids 1979;30:301.
[15] DeBruijn TJW, DeJong WA, Van Den Berg PJ. Thermochim Acta 1981;45:315.
[16] Málek J. Thermochim Acta 1995;267:61.
[17] Šesták J. Thermophysical properties of solids, their measurments and theoretical analysis. Amsterdam: Elsevier, 1984.
[18] Málek J. Thermochim Acta 1992;200:257.